

**Bright and Dark Quadrupolar Excitons in the WSe<sub>2</sub>/MoSe<sub>2</sub>/WSe<sub>2</sub> Heterotrilinear**Yongzhi Xie,<sup>1,\*</sup> Yuchen Gao,<sup>1,\*</sup> Fengyu Chen,<sup>2,\*</sup> Yunkun Wang,<sup>1</sup> Jun Mao,<sup>1</sup> Qinyun Liu,<sup>1</sup> Saisai Chu,<sup>1,3,4</sup>  
Hong Yang,<sup>1,3,4</sup> Yu Ye<sup>1,4</sup>,, Qihuang Gong,<sup>1,3,4</sup> Ji Feng<sup>2,5,†</sup> and Yunan Gao<sup>1,3,4,‡</sup><sup>1</sup>State Key Laboratory for Mesoscopic Physics and Frontiers Science Center for Nano-optoelectronics, School of Physics, Peking University, Beijing 100871, China<sup>2</sup>International Center for Quantum Materials, School of Physics, Peking University, Beijing 100871, China<sup>3</sup>Collaborative Innovation Center of Extreme Optics, Shanxi University, Taiyuan 030006, China<sup>4</sup>Peking University Yangtze Delta Institute of Optoelectronics, Nantong, Jiangsu 226010, China<sup>5</sup>Hefei National Laboratory, Hefei 230088, China

(Received 6 April 2023; accepted 25 September 2023; published 30 October 2023)

Transition metal dichalcogenide heterostructures have been extensively studied as a platform for investigating exciton physics. While heterobilayers such as WSe<sub>2</sub>/MoSe<sub>2</sub> have received significant attention, there has been comparatively less research on heterotrilinear, which may offer new excitonic species and phases, as well as unique physical properties. In this Letter, we present theoretical and experimental investigations on the emission properties of quadrupolar excitons (QXs), a newly predicted type of exciton, in a WSe<sub>2</sub>/MoSe<sub>2</sub>/WSe<sub>2</sub> heterotrilinear device. Our findings reveal that the optical brightness or darkness of QXs is determined by horizontal mirror symmetry and valley and spin selection rules. Additionally, the emission intensity and energy of both bright and dark QXs can be adjusted by applying an out-of-plane electric field, due to changes in hole distribution and the Stark effect. These results not only provide experimental evidence for the existence of QXs in heterotrilinear but also uncover their novel properties, which have the potential to drive the development of new exciton-based applications.

DOI: [10.1103/PhysRevLett.131.186901](https://doi.org/10.1103/PhysRevLett.131.186901)

Atomically thin transition metal dichalcogenide (TMD) layers exhibit a variety of stable excitons, including neutral excitons, charged excitons, biexcitons, interlayer excitons, etc. These excitons are formed due to reduced dielectric screening, resulting in higher binding energies [1–4]. Particularly, interlayer excitons in heterobilayers possess permanent dipoles, allowing for electrostatic control over their species, interactions, and motion. This characteristic enables the exploration of a rich array of excitonic physics [5–20]. Additionally, the coupling of spin and valley degrees of freedom in TMDs introduces new avenues for manipulating the interlayer twisting angle. This twisting angle gives rise to moiré potentials and leads to the emergence of various quantum phenomena, such as Wigner crystals, Hubbard model physics, correlated insulating states, stripe phases, and exciton insulators [21–33].

Extensive research has been conducted on TMD heterobilayers, and heterotrilinear incorporating TMDs, graphene, and hexagonal boron nitride (hBN) have also been reported [15,34]. However, heterotrilinear comprising three TMD monolayers remain relatively unexplored [35,36]. Recent theoretical predictions have highlighted the existence of a fascinating new type of exciton known as quadrupolar excitons (QXs), as illustrated in Fig. 1(a), along with the possibility of novel excitonic phases [37,38]. Currently, only a limited number of experimental studies have been conducted to confirm the existence of QXs and

investigate their properties [39–41]. In this Letter, we present theoretical and experimental evidence, along with new discoveries, regarding QXs in WSe<sub>2</sub>/MoSe<sub>2</sub>/WSe<sub>2</sub> heterotrilinear. Specifically, we demonstrate that QXs can exhibit optical bright or dark states, and we uncover their emission properties, which are primarily dictated by the structural symmetry and can be modified through the application of an out-of-plane electric field.

We begin with an examination of the recombination emission of QXs in the TMD heterotrilinear, from the symmetry viewpoint. In the monolayer case, the spin optical selection rules are valid due to the horizontal mirror symmetry, whereas this symmetry is broken in the heterobilayer that relaxes the optical selection rules [42]. In WSe<sub>2</sub>/MoSe<sub>2</sub> heterobilayer, dipole excitons (DXs) are known to be the brightest with twist angles near 0° (R stacking) and 60° (H stacking), because of zero momentum mismatch between interlayer valleys [43]. In WSe<sub>2</sub>/MoSe<sub>2</sub>/WSe<sub>2</sub> heterotrilinear, the horizontal mirror symmetry could be restored in HH and RR stacking, which enforces the spin optical selection rule:

$$\sigma_h(v)\sigma_h(c)e^{i\pi(S'_z-S_z)} = 1, \quad (1)$$

where  $\sigma_h(v)$  and  $\sigma_h(c)$  are the parity of valence and conduction states with respect to  $\sigma_h$ , respectively,  $\sigma_h$  is the horizontal reflection plane, and  $S'_z$  and  $S_z$  are the

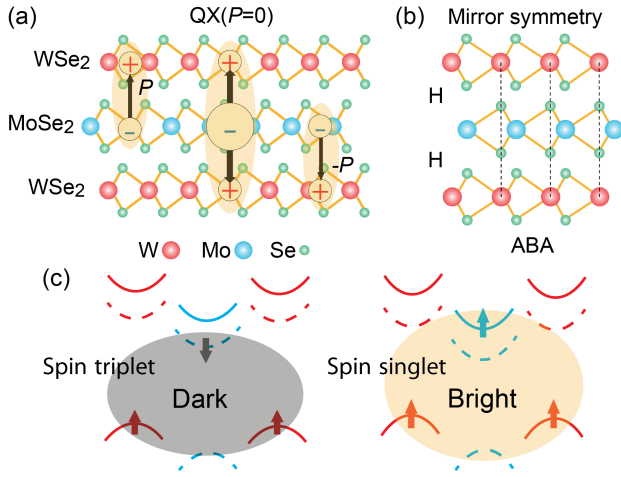


FIG. 1. (a) Illustration of the configuration of electrons and holes in WSe<sub>2</sub>/MoSe<sub>2</sub>/WSe<sub>2</sub> heterotrilaier. QXs or dipole excitons (DXs) exist in this system under zero or high electric fields. (b) HH-ABA stacking type of the heterotrilaier. (c) Optical selection rules caused by mirror symmetry are valid. The dark and bright QXs are shown in the schematic band diagrams, up and down arrows present the spin states of the electron and hole in the heterotrilaiers.

corresponding spin projections. In the WSe<sub>2</sub>/MoSe<sub>2</sub>/WSe<sub>2</sub> heterotrilaiers, it is well known that the valence band edges residing on the WSe<sub>2</sub> layers and the conduction band edges residing on the MoSe<sub>2</sub> layer can have different spin projections, depending on the stacking. Since  $\sigma_h(v) = \sigma_h(c) = +1$  for QXs, we may conclude that the QX is bright if the electron and hole have the same spin states, and dark otherwise; see Supplemental Material (SM) [44] for more explanation.

To restore mirror symmetry, in addition to the stacking type, the atomic arrangement must also be considered. In the HH stacking, the most energetically stable configuration is that the metal atoms align with the Se atoms, as illustrated in Fig. 1(b), forming HH-ABA atomic alignments [46–48]. HH-ABA has a horizontal mirror symmetry, so potential QXs of higher energy are bright owing to parallel electron and hole spins, i.e., spin-singlet interlayer excitons, whereas the lower energy QXs are spin-triplet interlayer excitons and dark [33], as depicted in Fig. 1(c). In this work, we limit ourselves to study the optical properties of WSe<sub>2</sub>/MoSe<sub>2</sub>/WSe<sub>2</sub> heterotrilaier with HH-ABA stacking.

To experimentally verify the optical bright and dark QXs and study their properties, we fabricated double-gated devices as shown in Fig. 2(a). The heterotrilaiers were prepared by dry transfer and tear-stacking technique [49], encapsulated by two nearly equal thickness hBN and grounded by a thin graphite. Two other graphites are used as the top gate and the bottom gate. The stacking configurations of the device were determined by the second harmonic generation measurement, which reveals the HH stacking of the device (see SM for details). Based on the

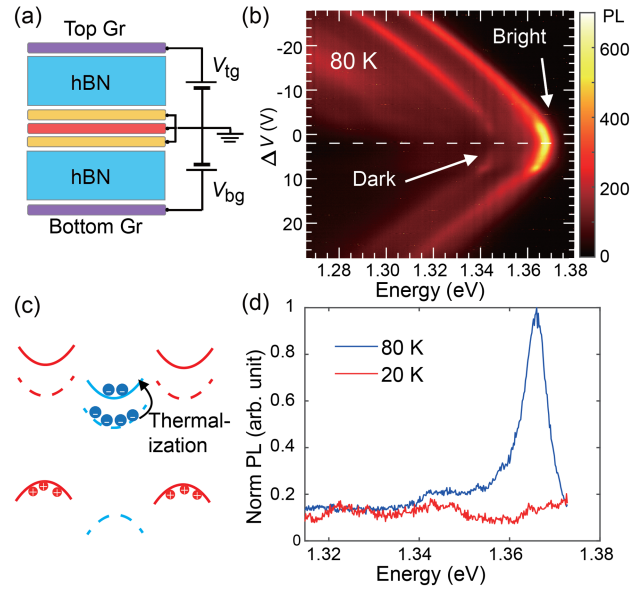


FIG. 2. (a) Schematic of the double-gate device.  $V_{tg}$  and  $V_{bg}$  denote the top gate voltage and bottom gate voltage, respectively. (b) Contour plot of the interlayer excitons emission intensity as a function of photon energy and gate voltage difference ( $\Delta V$ ). The doping of the heterotrilaier is controlled in the neutral region (see SM for details). The bright and dark states of QXs appear at a low electric field. (c) The sketch of charge distribution when the temperature changes. (d) Temperature dependent PL spectra of interlayer excitons in neutral doping when  $\Delta V = 2$  V. The PL intensity of bright QXs vanishes when temperature changes from 80 to 20 K due to the temperature dependent thermalization.

parallel-plate capacitor model, the out-of-plane electric field  $F$  is controlled by  $\Delta V = V_{tg} - V_{bg}$ ,  $F = \Delta V / (d_{t-hBN} + d_{b-hBN})$ , and the total electronic doping of the trilaier is  $n_e \propto V_{tg} / d_{(t-hBN)} + V_{bg} / d_{(b-hBN)}$ , where  $V_{tg}$ ,  $V_{bg}$  are the voltage of the top and bottom gates, and  $d_{t-hBN}$ ,  $d_{b-hBN}$  are the thickness of the top hBN (53 nm) and bottom hBN (63 nm). The photoluminescence (PL) spectra of the heterotrilaier as a function of gate-voltage difference were measured at 80 K and presented in Fig. 2(b), in which two parallel hyperbolic emission curves can be noticeably seen.

Under the near-zero electric field ( $\Delta V = 2$  V), the hole amplitudes in the upper and lower WSe<sub>2</sub> are symmetric. Along the dashed line in Fig. 2(b), it can be seen that one emission curve gives the highest intensity while the other one is almost completely dark. This striking intensity difference supplies the first intuitive evidence of optical bright and dark DXs speculated from the valley-spin optical selection rules as illustrated in Fig. 1(c) that the spin-singlet (spin-triplet) QXs are spin-allowed (spin-forbidden). To further support our interpretation, we lower the temperature from 80 to 20 K, since the bright QXs require electrons occupying the higher levels via thermalization, as depicted in Fig. 2(c). As shown in Fig. 2(d), decreasing the temperature indeed quenches the bright QX emission.

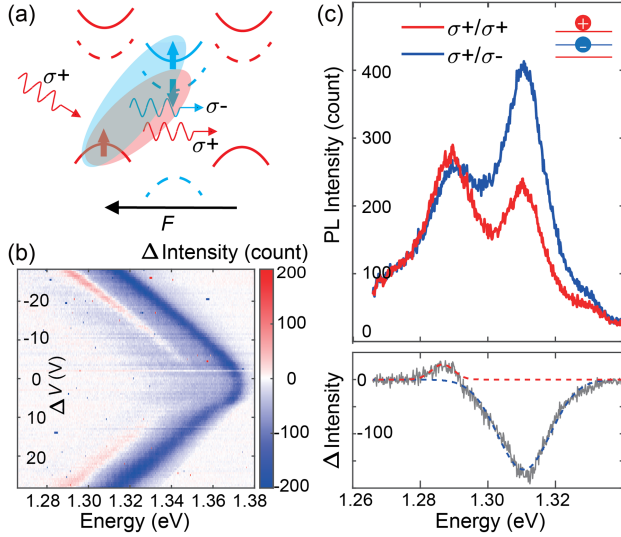


FIG. 3. (a) Different valley polarization for spin-singlet and spin-triplet quadrupolar excitons. (b) Contour plot of  $\Delta I = I_{\sigma^+} - I_{\sigma^-}$  with  $\sigma^+$  excitation as a function of emission energy and gate-voltage difference ( $\Delta V$ ) in the neutral doping region at 80 K; spin-singlet and spin-triplet quadrupolar excitons show different valley polarization. (c) Valley polarization PL spectra of quadrupolar excitons at  $\Delta V = 28$  V.

Next, we analyze the PL spectra variation under external electric field. The dependence of the overall spectra on the electric field will be quantitatively analyzed later using a coupling model, whereas here we focus on further verification of the assignment of optical dark and bright QXs. When the electric field increases, it can be seen in Fig. 2(b) the dark QXs brighten, owing to that the electric field shifts the hole distribution and breaks the horizontal symmetry and relaxes the emission prohibition as illustrated in Fig. 3(a). The energy difference between two emission curves is 23 meV, which is the same as the reported value of the splitting of conduction bands of  $\text{MoSe}_2$  caused by the spin-orbit coupling [33], providing convincing qualitative evidence of our assignment. Under a higher electric field, the hyperbolic emission curves transition toward linear lines, resembling the behavior observed in the Stark effect. This occurs because the electric field causes a more concentrated distribution of holes in one layer of  $\text{WSe}_2$ . Consequently, the interlayer excitons exhibit behavior that is effectively similar to a DX. The Stark coefficient is determined as  $|\alpha| = 0.29 \text{ e} \times \text{nm}$  and a 0.54 nm separation of electron and hole is extracted, which is consistent with the result of heterobilayer [17,18] and indicate good interlayer coupling in our device.

Further evidence of the spin triplet (spin singlet) of optical dark (bright) QXs is the valley polarization of the interlayer excitons, as sketched in Fig. 3(a). The excitation photon energy is chosen at 1.713 eV to resonantly excite  $\text{WSe}_2$  for its long hole spin life [18]. Figure 3(b) shows the PL intensity difference  $\Delta I = I_{\sigma^+} - I_{\sigma^-}$  with  $\sigma^+$  excitation as

a function of emission energy and gate voltage difference. Different signs of valley polarization in the high-energy state and the low-energy state are observed, which confirm the spin configurations of the two states shown in Fig. 3(a), that is, the low-energy state is a spin-triplet exciton, and the high-energy state is a spin-singlet exciton. Typical valley polarization PL spectra under a large electric field of  $\Delta V = 28$  V are shown in Fig. 3(c), in which the valley polarization  $(I_{\sigma^+} - I_{\sigma^-}) / (I_{\sigma^+} + I_{\sigma^-})$  is about  $-30\%$  for the spin-singlet excitons and about  $10\%$  for the spin-triplet excitons. Valley polarization in TMD heterobilayers has been well-explained in literature such as Ref. [33], so the measured valley polarization provides another convincing evidence for the spin configuration of the heterotrilayers as we proposed in Fig. 1(c).

A theoretical model can be constructed to describe the forming and emission properties of observed QXs. As shown above, the QX emission can be tuned by an out-of-plane electric field, showing a hyperbolic dependence of the emission energy on the electric field that is the typical feature of a two-level system with coupling. We assume that the upper and lower  $\text{WSe}_2$  layers are related by mirror reflection,  $\sigma_h$ , and the hole states entering into the exciton are a linear combination of the upper and lower hole states  $\psi_{\text{hu}}^0, \psi_{\text{hl}}^0$ . To account for the out-of-plane electric field  $F$  that lifts the degeneracy between  $\psi_{\text{hu}}^0$  and  $\psi_{\text{hl}}^0$ , and the hopping between them, a minimal two-level Hamiltonian can be written as

$$H = \begin{bmatrix} \alpha F & -t \\ -t & -\alpha F \end{bmatrix}, \quad (2)$$

where  $\alpha$  is the Stark coefficient, and the hopping amplitude  $t$  is taken to be constant. The hybridized hole state energy and wave function are

$$\varepsilon = +\sqrt{t^2 + \alpha^2 F^2}, \quad \psi_h^0 = A\psi_{\text{hu}}^0 + B\psi_{\text{hl}}^0, \quad (3)$$

where  $A$  and  $B$  are the amplitudes of the hole wave function in the top and bottom  $\text{WSe}_2$  layers, respectively. The optical matrix element is then

$$\langle \psi_h | \hat{p}_+ | \psi_e \rangle = p(A + B), \quad (4)$$

where the matrix element  $p = \langle \psi_{\text{hu}}^0 | \hat{p}_+ | \psi_e^0 \rangle = \langle \psi_{\text{hl}}^0 | \hat{p}_+ | \psi_e^0 \rangle$ , due to the transformation  $\sigma_h \psi_{\text{hl}} = \psi_{\text{hu}}$  and vice versa. Accordingly, the PL intensity is proportional to  $|A + B|^2$  [50]. It is worth mentioning that the optical matrix element  $p$  has to be distinguished from the permanent dipole moments  $P$  of 0 for quadrupolar excitons. The permanent dipole moment is determined by the electrostatic charge distribution, while the optical matrix elements are related to the transient displacement of the electron and hole wave functions. This difference has been explained in TMD heterobilayer, where the interlayer excitons having

permanent dipole moments in the normal direction of the heterobilayer show dominant in-plane optical transition dipoles [51].

Equation (3) shows that the emission center  $\varepsilon$  as a function of the electric field has a hyperbolic dependence. In addition, the theory model tells that the emission attains the highest intensity at zero fields, where the hole is an equal-weight hybridization of upper and lower hole states. The highest intensity is twice as the lowest intensity in this model. Although we have ignored the Coulomb interaction in the formation of excitons, the above analysis provides a zeroth-order description of the PL intensity of QXs, which in combination with the symmetry considerations above will facilitate our optical measurements.

Considering that the PL emission of dark QXs (spin-triplet excitons) vanishes at small electric field, we extract PL data of the bright one (spin-singlet excitons) in Fig. 2(b) by Gaussian fitting. The fitting peak energy as a function of the electric field is shown in Fig. 4(a). The derived hyperbolic dependence from the two-level Hamiltonian model agrees well with the experimental data. A hopping strength  $t = 16$  meV is extracted, which is within the theory predicted range [37]. Under higher electric field, the hyperbola is close to the asymptotic line, suggesting that holes mainly gather only in one of the WSe<sub>2</sub> layers, as shown by the inset of Fig. 3(a).

The normalized intensities of bright QXs, shown in Fig. 4(b), show about a twofold change at high and zero electric fields, which is semiquantitatively consistent with the theoretical model, although not as perfectly so as the emission energy dependence is. As for the intensity, the key factor is the optical matrix element  $\langle \psi_{\text{hu}}^0 | \hat{p}_+ | \psi_{\text{e}}^0 \rangle$ , but it can also be affected by other imperfect factors in the TMDs, such as other decay paths. To inspect the optical matrix element, one way is to measure the decay rate of the excitons. According to the Fermi's golden rule, the decay lifetime is inversely proportional to the square of optical matrix element. The time-resolved PL (TRPL) traces at  $\Delta V = 0, 5, 10$  V are shown in Fig. 4(c), where multiple decay components can be seen. The lifetime of the component sensitive to the electric field is extracted and shown in Fig. 4(d). Because the linear Stark effect also influences the lifetime of interlayer excitons, we limit the selection of electric field regions ( $0 \leq \Delta V \leq 10$ ) to those where the changes in interlayer exciton energy are relatively small. A long-pass filter and a short-pass filter are used to pick the PL of spin-singlet QXs. It can be seen that the intensity extracted by TRPL shows good agreement with steady-state results that shorter lifetime corresponds to higher PL intensity. The lifetime trend of QXs also agrees semiquantitatively with the theoretical model. The good agreement between the theoretical model and steady-state PL and TRPL verifies that the electric field indeed controls the overlap of electron and hole wave functions in the heterotrilyer, actively modulating the emission properties

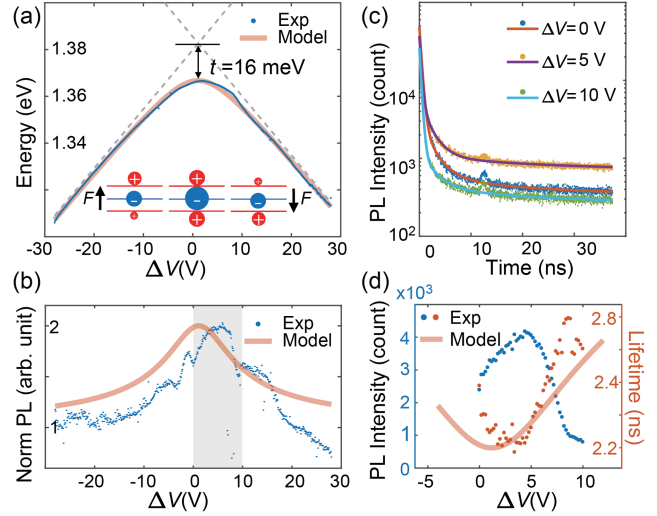


FIG. 4. (a) Extracted peak energy of higher energy interlayer excitons in Fig. 2(b) by Gaussian fitting. Solid line is a minimal two-level Hamiltonian model fitting. A hopping amplitude of 16 meV is given. (b) Normalized integrated PL intensity of higher energy interlayer excitons and results of theory model. The inset indicates the distribution of electrons and holes under the different electric fields.  $F$  is the external out-of-plane electric field. (c) Time-resolved PL of higher energy interlayer excitons at different  $\Delta V$ . The solid lines are the fit results using the triple exponential function. (d) Extracted lifetime and strength of the field-sensitive component as a function of the field strength. The theoretical model qualitatively represents the experimental data.

of QXs in the device. To note, there is a small discrepancy that the highest intensity occurs at  $\Delta V \approx 5$  V rather than the center of the hyperbola  $\Delta V \approx 2$  V. We attribute this to the different sensitivities of emission energy and intensity on imperfect factors in the device and in the TMDs.

In summary, this work provides experimental observations of theoretically predicted QX in the WSe<sub>2</sub>/MoSe<sub>2</sub>/WSe<sub>2</sub> heterotrilyers. Moreover, we found they can be optical bright or dark determined by the mirror symmetry and related spin selection rules. By shifting the distribution of hole wave function using an out-of-plane electric field, the emission properties of both bright and dark QXs can be modulated. The heterotrilyers would be a fertile platform for exploring complex excitonic phases and quantum states, and may also have potential applications in optoelectronics, as their properties can be controlled either electrically or by stacking structures.

This work is supported by the National Key Research and Development Program of China (Grants No. 2021YFA1400100, No. 2018YFA0306302, and No. 2018YFA0305601), and the National Natural Science Foundation of China (NSFC, Grants No. 92250305, No. 12274003, and No. 11934001). J.F. acknowledges the support by the Innovation Program for Quantum Science and Technology (Grant No. 2021ZD0302600).

Yunan Gao acknowledges the support by the Fundamental Research Funds for the Central Universities.

\*These authors contributed equally to this work.

<sup>†</sup>Corresponding author: jfeng11@pku.edu.cn

<sup>‡</sup>Corresponding author: gyn@pku.edu.cn

- [1] A. Chernikov, T. C. Berkelbach, H. M. Hill, A. Rigosi, Y. Li, B. Aslan, D. R. Reichman, M. S. Hybertsen, and T. F. Heinz, *Phys. Rev. Lett.* **113**, 076802 (2014).
- [2] K. F. Mak, K. He, C. Lee, G. H. Lee, J. Hone, T. F. Heinz, and J. Shan, *Nat. Mater.* **12**, 207 (2013).
- [3] Z. Li, T. Wang, Z. Lu, C. Jin, Y. Chen, Y. Meng, Z. Lian, T. Taniguchi, K. Watanabe, S. Zhang, D. Smirnov, and S.-F. Shi, *Nat. Commun.* **9**, 3719 (2018).
- [4] F. Ceballos, M. Z. Bellus, H.-Y. Chiu, and H. Zhao, *ACS Nano* **8**, 12717 (2014).
- [5] F. Vialla, M. Danovich, D. A. Ruiz-Tijerina, M. Massicotte, P. Schmidt, T. Taniguchi, K. Watanabe, R. J. Hunt, M. Szyniszewski, N. D. Drummond, T. G. Pedersen, V. I. Fal'ko, and F. H. L. Koppens, *2D Mater.* **6**, 035032 (2019).
- [6] Z. Wang, Y.-H. Chiu, K. Honz, K. F. Mak, and J. Shan, *Nano Lett.* **18**, 137 (2018).
- [7] Z. Huang, Y. Liu, K. Dini, Q. Tan, Z. Liu, H. Fang, J. Liu, T. Liew, and W. Gao, *Nano Lett.* **20**, 1345 (2020).
- [8] D. Unuchek, A. Ciarrocchi, A. Avsar, K. Watanabe, T. Taniguchi, and A. Kis, *Nature (London)* **560**, 340 (2018).
- [9] E. Liu, E. Barré, J. van Baren, M. Wilson, T. Taniguchi, K. Watanabe, Y.-T. Cui, N. M. Gabor, T. F. Heinz, Y.-C. Chang, and C. H. Lui, *Nature (London)* **594**, 46 (2021).
- [10] Y. Meng, T. Wang, C. Jin, Z. Li, S. Miao, Z. Lian, T. Taniguchi, K. Watanabe, F. Song, and S.-F. Shi, *Nat. Commun.* **11**, 2640 (2020).
- [11] W. Li, X. Lu, S. Dubey, L. Devenica, and A. Srivastava, *Nat. Mater.* **19**, 624 (2020).
- [12] J. Sung, Y. Zhou, G. Scuri, V. Zólyomi, T. I. Andersen, H. Yoo, D. S. Wild, A. Y. Joe, R. J. Gelly, H. Heo, S. J. Magorrian, D. Bérubé, A. M. M. Valdivia, T. Taniguchi, K. Watanabe, M. D. Lukin, P. Kim, V. I. Fal'ko, and H. Park, *Nat. Nanotechnol.* **15**, 750 (2020).
- [13] Y. Tang, J. Gu, S. Liu, K. Watanabe, T. Taniguchi, J. Hone, K. F. Mak, and J. Shan, *Nat. Nanotechnol.* **16**, 52 (2021).
- [14] H. Baek, M. Brotons-Gisbert, A. Campbell, V. Vitale, J. Lischner, K. Watanabe, T. Taniguchi, and B. D. Gerardot, *Nat. Nanotechnol.* **16**, 1237 (2021).
- [15] A. Ciarrocchi, D. Unuchek, A. Avsar, K. Watanabe, T. Taniguchi, and A. Kis, *Nat. Photonics* **13**, 131 (2019).
- [16] Z. Sun, A. Ciarrocchi, F. Tagarelli, J. F. Gonzalez Marin, K. Watanabe, T. Taniguchi, and A. Kis, *Nat. Photonics* **16**, 79 (2022).
- [17] L. A. Jauregui, A. Y. Joe, K. Pistunova, D. S. Wild, A. A. High, Y. Zhou, G. Scuri, K. D. Greve, A. Sushko, C.-H. Yu, T. Taniguchi, K. Watanabe, D. J. Needleman, M. D. Lukin, H. Park, and P. Kim, *Science* **366**, 870 (2019).
- [18] X. Wang, J. Zhu, K. L. Seyler, P. Rivera, H. Zheng, Y. Wang, M. He, T. Taniguchi, K. Watanabe, J. Yan, D. G. Mandrus, D. R. Gamelin, W. Yao, and X. Xu, *Nat. Nanotechnol.* **16**, 1208 (2021).
- [19] Y. Zhang, C. Xiao, D. Ovchinnikov, J. Zhu, X. Wang, T. Taniguchi, K. Watanabe, J. Yan, W. Yao, and X. Xu, *Nat. Nanotechnol.* **18**, 501 (2023).
- [20] P. Rivera, H. Yu, K. L. Seyler, N. P. Wilson, W. Yao, and X. Xu, *Nat. Nanotechnol.* **13**, 1004 (2018).
- [21] E. M. Alexeev, D. A. Ruiz-Tijerina, M. Danovich, M. J. Hamer, D. J. Terry, P. K. Nayak, S. Ahn, S. Pak, J. Lee, J. I. Sohn, M. R. Molas, M. Koperski, K. Watanabe, T. Taniguchi, K. S. Novoselov, R. V. Gorbachev, H. S. Shin, V. I. Fal'ko, and A. I. Tartakovskii, *Nature (London)* **567**, 81 (2019).
- [22] C. Jin, E. C. Regan, A. Yan, M. Iqbal Bakti Utama, D. Wang, S. Zhao, Y. Qin, S. Yang, Z. Zheng, S. Shi, K. Watanabe, T. Taniguchi, S. Tongay, A. Zettl, and F. Wang, *Nature (London)* **567**, 76 (2019).
- [23] K. L. Seyler, P. Rivera, H. Yu, N. P. Wilson, E. L. Ray, D. G. Mandrus, J. Yan, W. Yao, and X. Xu, *Nature (London)* **567**, 66 (2019).
- [24] K. Tran *et al.*, *Nature (London)* **567**, 71 (2019).
- [25] C. Jin, E. C. Regan, D. Wang, M. Iqbal Bakti Utama, C.-S. Yang, J. Cain, Y. Qin, Y. Shen, Z. Zheng, K. Watanabe, T. Taniguchi, S. Tongay, A. Zettl, and F. Wang, *Nat. Phys.* **15**, 1140 (2019).
- [26] J. Choi, M. Florian, A. Steinhoff, D. Erben, K. Tran, D. S. Kim, L. Sun, J. Quan, R. Claassen, S. Majumder, J. A. Hollingsworth, T. Taniguchi, K. Watanabe, K. Ueno, A. Singh, G. Moody, F. Jahnke, and X. Li, *Phys. Rev. Lett.* **126**, 047401 (2021).
- [27] E. C. Regan, D. Wang, C. Jin, M. I. Bakti Utama, B. Gao, X. Wei, S. Zhao, W. Zhao, Z. Zhang, K. Yumigeta, M. Blei, J. D. Carlström, K. Watanabe, T. Taniguchi, S. Tongay, M. Crommie, A. Zettl, and F. Wang, *Nature (London)* **579**, 359 (2020).
- [28] Y. Tang, L. Li, T. Li, Y. Xu, S. Liu, K. Barmak, K. Watanabe, T. Taniguchi, A. H. MacDonald, J. Shan, and K. F. Mak, *Nature (London)* **579**, 353 (2020).
- [29] Y. Xu, S. Liu, D. A. Rhodes, K. Watanabe, T. Taniguchi, J. Hone, V. Elser, K. F. Mak, and J. Shan, *Nature (London)* **587**, 214 (2020).
- [30] C. Jin, Z. Tao, T. Li, Y. Xu, Y. Tang, J. Zhu, S. Liu, K. Watanabe, T. Taniguchi, J. C. Hone, L. Fu, J. Shan, and K. F. Mak, *Nat. Mater.* **20**, 940 (2021).
- [31] J. Gu, L. Ma, S. Liu, K. Watanabe, T. Taniguchi, J. C. Hone, J. Shan, and K. F. Mak, *Nat. Phys.* **18**, 395 (2022).
- [32] Z. Zhang, E. C. Regan, D. Wang, W. Zhao, S. Wang, M. Sayyad, K. Yumigeta, K. Watanabe, T. Taniguchi, S. Tongay, M. Crommie, A. Zettl, M. P. Zaletel, and F. Wang, *Nat. Phys.* **18**, 1214 (2022).
- [33] T. Wang, S. Miao, Z. Li, Y. Meng, Z. Lu, Z. Lian, M. Blei, T. Taniguchi, K. Watanabe, S. Tongay, D. Smirnov, and S.-F. Shi, *Nano Lett.* **20**, 694 (2020).
- [34] D. Unuchek, A. Ciarrocchi, A. Avsar, Z. Sun, K. Watanabe, T. Taniguchi, and A. Kis, *Nat. Nanotechnol.* **14**, 1104 (2019).
- [35] F. Ceballos, M.-G. Ju, S. D. Lane, X. C. Zeng, and H. Zhao, *Nano Lett.* **17**, 1623 (2017).
- [36] H. Zheng, B. Wu, S. Li, J. Ding, J. He, Z. Liu, C.-T. Wang, J.-T. Wang, A. Pan, and Y. Liu, *Light Sci. Appl.* **12**, 117 (2023).
- [37] Y. Slobodkin, Y. Mazuz-Harpaz, S. Refaely-Abramson, S. Gazit, H. Steinberg, and R. Rapaport, *Phys. Rev. Lett.* **125**, 255301 (2020).

- [38] G. E. Astrakharchik, I. L. Kurbakov, D. V. Sychev, A. K. Fedorov, and Y. E. Lozovik, *Phys. Rev. B* **103**, L140101 (2021).
- [39] Y. Bai, Y. Li, S. Liu, Y. Guo, J. Pack, J. Wang, C. R. Dean, J. Hone, and X. Y. Zhu, [arXiv:2207.09601v3](https://arxiv.org/abs/2207.09601v3).
- [40] W. Li, Z. Hadjri, J. Zhang, L. M. Devenica, S. Liu, J. Hone, K. Watanabe, T. Taniguchi, A. Rubio, and A. Srivastava, [arXiv:2208.05490](https://arxiv.org/abs/2208.05490).
- [41] Z. Lian, D. Chen, L. Ma, Y. Meng, Y. Su, L. Yan, X. Huang, Q. Wu, X. Chen, M. Blei, T. Taniguchi, K. Watanabe, S. Tongay, C. Zhang, Y.-T. Cui, and S.-F. Shi, *Nat. Commun.* **14**, 4604 (2023).
- [42] H. Yu, G.-B. Liu, and W. Yao, *2D Mater.* **5**, 035021 (2018).
- [43] P. K. Nayak, Y. Horbatenko, S. Ahn, G. Kim, J.-U. Lee, K. Y. Ma, A.-R. Jang, H. Lim, D. Kim, S. Ryu, H. Cheong, N. Park, and H. S. Shin, *ACS Nano* **11**, 4041 (2017).
- [44] See Supplemental Material at <http://link.aps.org/supplemental/10.1103/PhysRevLett.131.186901> for optical selection rules for quadrupolar excitons, sample fabrication, SHG measurements, methods of PL measurements, doping dependence PL spectra and temperature dependent PL spectra of interlayer excitons at large electric field, which includes Ref. [45].
- [45] W.-T. Hsu, Z.-A. Zhao, L.-J. Li, C.-H. Chen, M.-H. Chiu, P.-S. Chang, Y.-C. Chou, and W.-H. Chang, *ACS Nano* **8**, 2951 (2014).
- [46] S. Carr, D. Massatt, S. B. Torrisi, P. Cazeaux, M. Luskin, and E. Kaxiras, *Phys. Rev. B* **98**, 224102 (2018).
- [47] Z. Zhu, P. Cazeaux, M. Luskin, and E. Kaxiras, *Phys. Rev. B* **101**, 224107 (2020).
- [48] V. V. Enaldiev, V. Zólyomi, C. Yelgel, S. J. Magorrian, and V. I. Fal'ko, *Phys. Rev. Lett.* **124**, 206101 (2020).
- [49] D. G. Purdie, N. M. Pugno, T. Taniguchi, K. Watanabe, A. C. Ferrari, and A. Lombardo, *Nat. Commun.* **9**, 5387 (2018).
- [50] H. B. Bebb and E. W. Willams, *Chapter 4 Photoluminescence I: Theory, in Semiconductors and Semimetals* (1972), Vol. 8, 10.1016/S0080-8784(08)62345-5.
- [51] L. Sigl, M. Troue, M. Katzer, M. Selig, F. Sigger, J. Kiemle, M. Brotons-Gisbert, K. Watanabe, T. Taniguchi, B. D. Gerardot, A. Knorr, U. Wurstbauer, and A. W. Holleitner, *Phys. Rev. B* **105**, 035417 (2022).